

## New ZnSnO<sub>3</sub>-based varistor system

G. Z. ZANG, J. F. WANG, H. C. CHEN, W. B. SU, W. X. WANG, P. QI, C. M. WANG  
 School of Physics and Microelectronics, State Key Laboratory of Crystal Materials, Shandong University,  
 Jinan 250100, People's Republic of China  
 E-mail: zanggouxhong@sina.com

Semiconducting ceramics are widely used in electrical industries involving mobile communications, computers, signal processing, power transport, and control systems, because of their unique and useful electrical characteristics [1]. Varistors which are generally used to protect electronic circuits from voltage shock can sense and limit high transient voltage surges and can repeatedly endure such surges without being destroyed. The most important property of a varistor is its nonlinear voltage–current characteristic. It can be expressed by the equation  $I = KV^\alpha$ . The  $\alpha$  coefficient gives the degree of nonlinearity and the constant  $K$  depends on the microstructure and is related to the electrical resistivity of the material.

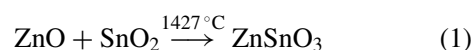
Commercial varistors used in protection systems are based on SiC or on ZnO. Varistors based on SiC have low nonlinearity coefficients [2–4] and ZnO varistors exhibit high nonlinear coefficients, but the degradation problem of ZnO varistors has not been resolved [5–7]. Therefore, the efforts to find new varistor materials have been ongoing. In 1983, N. Yumaka, M. Masuyama found that SrTiO<sub>3</sub>-based ceramics made by a two-step process had varistor characteristics [8]. In 1995, S. A. Pianaro found a new varistor material [4], (Co,Nb)-doped SnO<sub>2</sub>, which has only a single phase, rutile structure. In 2000, J. F. Wang found one oxide (Sb<sub>2</sub>O<sub>3</sub>)-doped TiO<sub>2</sub> ceramic to have varistor behavior [9]. Following Wang, W. B. Su found, in 2002, another TiO<sub>2</sub> varistor doped with only one oxide (WO<sub>3</sub>) [10].

In this work, we found a new varistor material, (Nb,Si)-doped ZnSnO<sub>3</sub>, and investigated the effects of SiO<sub>2</sub> on the properties of the (Nb,Si)-doped ZnSnO<sub>3</sub> varistor.

The materials used were analytical grades of SnO<sub>2</sub> (99.5%), Nb<sub>2</sub>O<sub>5</sub> (99.5%), ZnO (99.5%), and SiO<sub>2</sub> (90.0%). The compositions were SnO<sub>2</sub> + ZnO + 0.2%Nb<sub>2</sub>O<sub>5</sub> +  $x$ %SiO<sub>2</sub> in molar terms, where  $x = 0, 0.25, 0.4, 0.5, 1.0$ . The varistors were prepared by conventional ceramic processing. The mixed raw chemicals were milled in a nylon kettle with ZrO<sub>2</sub> balls and some distilled water, dried, mixed with 0.6% weight of PVA binder and pressed into disks 15 mm in diameter and 1.5 mm in thickness at 160 MPa. The disks were sintered at 1427 °C for an hour and cooled to room temperature after burning out the PVA binder at 650 °C. To measure the electrical properties, silver electrodes were made on both surfaces of the sintered disks. For microstructure characterization, the surfaces of the samples were observed by scanning electron microscopy (SEM) and the phases were analyzed by

X-ray diffraction (XRD). For electrical characterization of current density versus applied electrical field, an I–V grapher (QT2) was used. The complex impedance dependent on frequency is measured using an Agilent 4294A impedance analyzer.

According to the XRD analysis (Fig. 1), no apparent second phase was observed and SnO<sub>2</sub> and ZnO should be synthesized according to the following reaction [11]:



The electrical nonlinear characteristics of the samples are shown in Figs 2 and 3. The nonlinear coefficients  $\alpha$  which are shown in Table I are calculated by the following equation [4, 11]:

$$\alpha = \frac{\log(I_2/I_1)}{\log(V_2/V_1)} \quad (2)$$

where  $V_1$  and  $V_2$  are the voltages at currents  $I_1$  and  $I_2$ , respectively. It is found obviously from Figs 2 and 3 that the breakdown electrical field  $E_b$  of the varistor without SiO<sub>2</sub> is much higher than that of the varistors with different contents of SiO<sub>2</sub> dopant.

The microstructure of the samples doped without SiO<sub>2</sub> and with 0.4 mol% SiO<sub>2</sub> is shown in Figs 4 and 5. One can find some flaws on the surface of the sample without SiO<sub>2</sub>. The flaws might be produced by the internal uneven stresses caused by cooling.

Potential barrier height of the grain boundaries is measured according to the following equation [13, 14]:

$$J_S = AT^2 \exp\left[\frac{\beta\sqrt{E} - \phi_B}{k_B T}\right] \quad (3)$$

where  $A$  is the Richardson constant,  $k_B$  is the Boltzman constant,  $\phi_B$  is the barrier height,  $E$  is the electrical field, and  $\beta$  is a constant determined by the relation

$$\beta = \sqrt{\frac{1}{n\omega} \left( \frac{2e^3}{4\pi\epsilon_r\epsilon_0} \right)} \quad (4)$$

where  $n$  is the grain number per unit length,  $\omega$  is the barrier width,  $e$  is the electron charge, and  $\epsilon_r$  is the relative permittivity.  $J$  and  $E$  of some of the samples were measured at different temperatures. The value of  $\phi_B$  of the varistor without SiO<sub>2</sub> is much higher than that of the varistors with different contents of SiO<sub>2</sub> dopant as shown in Table I.

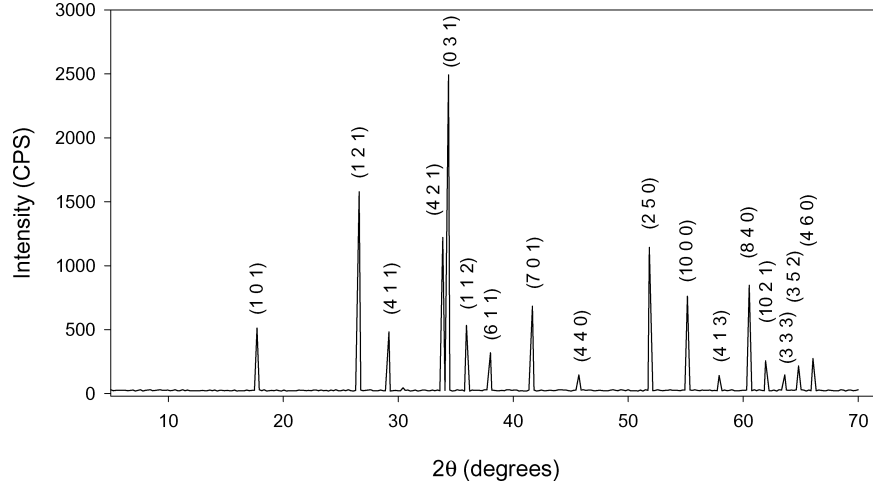


Figure 1 X-ray diffraction pictures for a sample doped with 0.4 mol% SiO<sub>2</sub>.

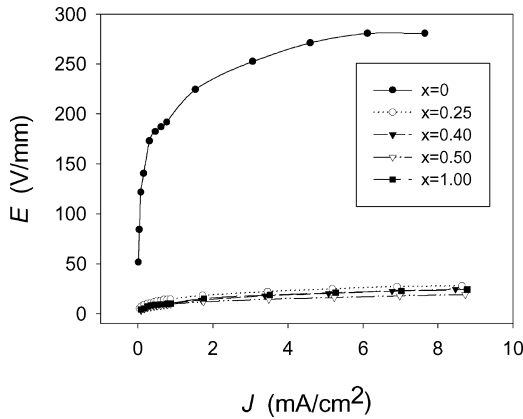


Figure 2 Electrical field applied vs. current density for samples with different SiO<sub>2</sub> contents.

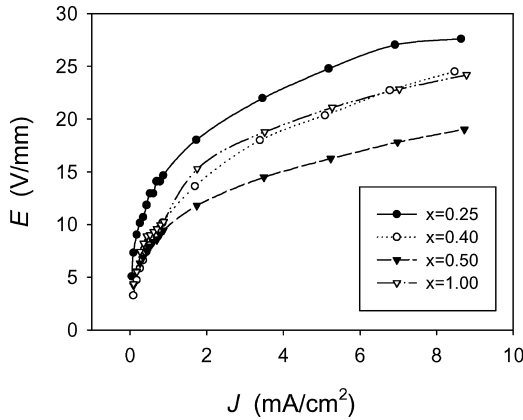
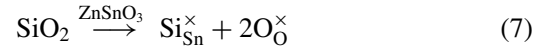
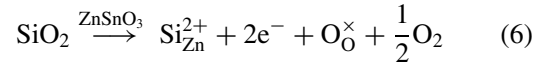
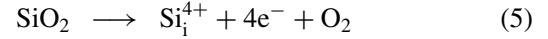


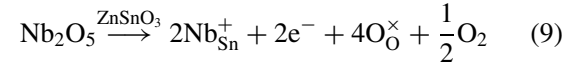
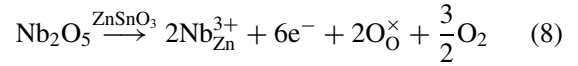
Figure 3 Electrical field applied vs. current density for samples with different SiO<sub>2</sub> contents.

Figs 6 and 7 show the complex impedance spectra of the varistors without SiO<sub>2</sub> and with 0.4 mol% SiO<sub>2</sub>. It is found clearly that the resistance of the former is much higher than that of the latter at low frequency (40 Hz) and high frequency (15 MHz), respectively. This indicates that SiO<sub>2</sub> may have increased the electronic conductivity of the ZnSnO<sub>3</sub> grains and grain boundaries since the polycrystalline ceramic is often considered as a large number of capacitors in series [15]. So the

addition of SiO<sub>2</sub> may lead to the following reactions:



The addition of Nb<sub>2</sub>O<sub>5</sub> to the ZnSnO<sub>3</sub>-based varistors may lead to the following reactions:



The Si<sub>i</sub><sup>4+</sup> located at the interstitial of ZnSnO<sub>3</sub> lattice and the e<sup>-</sup> originated in the above reaction will increase the electrical conductivity of the varistors. The higher electronic conductivity and lower potential barrier height of the varistors doped with SiO<sub>2</sub> may be the main reason for their lower breakdown electrical field than that of the varistor without SiO<sub>2</sub>. Some of the e<sup>-</sup> originated in Equations 5, 6, 8, and 9 will be captured by the oxygen partly absorbed at ZnSnO<sub>3</sub> grain boundaries.

The varistor behavior of ZnSnO<sub>3</sub> can be explained by the introduction of defects in the crystal lattice that are responsible for the formation of Schottky-type potential barriers at the grain boundaries. By analogy to the atomic defect model proposed by Gupta [16] for the ZnO varistor, the potential barrier is formed by

TABLE I Characteristics of the samples doped with different contents of SiO<sub>2</sub>

SiO <sub>2</sub> (mol%)	α	Density (g/cm <sup>3</sup> )	E <sub>b</sub> (V/mm)	φ <sub>B</sub> (eV)
0	6.0	5.28	198	0.84
0.25	3.6	6.28	14.6	0.74
0.40	2.0	6.01	10.2	0.78
0.50	3.3	6.28	7.9	0.72
1.00	2.7	6.18	11.8	0.73

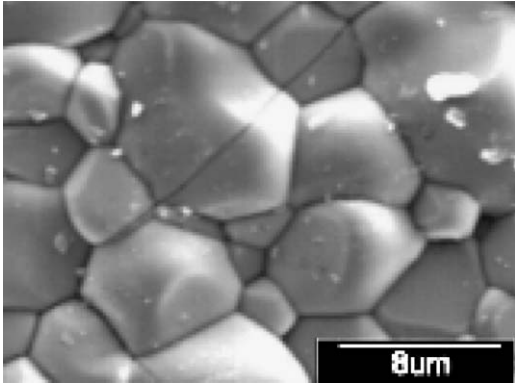


Figure 4 SEM photomicrographs of a sample doped without SiO<sub>2</sub>.

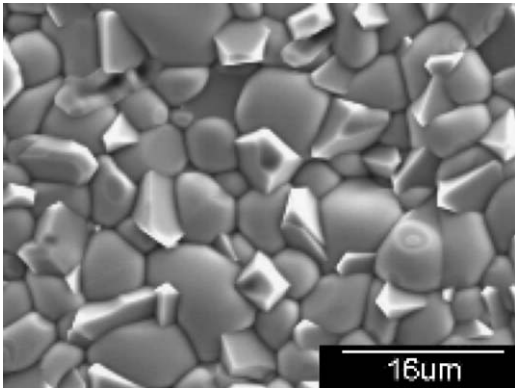


Figure 5 SEM photomicrographs of a sample doped with 0.4 mol% SiO<sub>2</sub>.

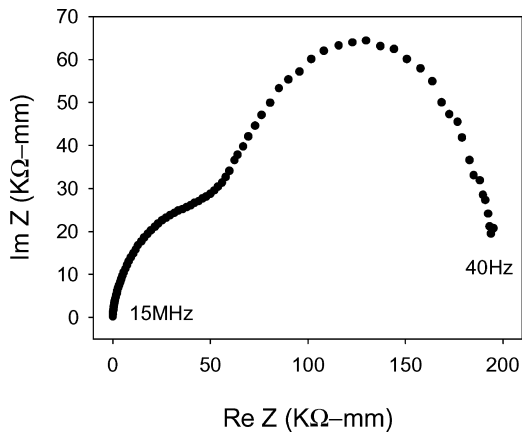


Figure 6 Complex impedance spectra of a sample doped without SiO<sub>2</sub>.

intrinsic defects of ZnSnO<sub>3</sub>, extrinsic defects created by solid substitution of dopants, and negative charges at the interface corresponding to vacancies of tin and zinc atoms. These defects create depletion layers at grain boundaries leading to the formation of a voltage barrier for the electronic transport. This transport occurs by tunneling and is responsible for the nonlinear

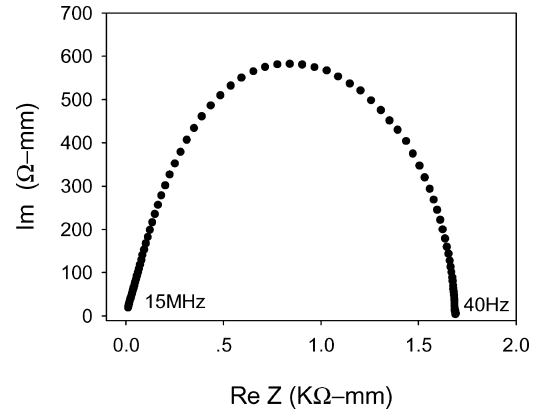


Figure 7 Complex impedance spectra of a sample doped with 0.4 mol% SiO<sub>2</sub>.

behavior of current density versus applied electric field [17].

The values of the nonlinear coefficients  $\alpha$  of the varistors obtained in this study are low. Efforts to further improve the nonlinear coefficient  $\alpha$  are in progress.

#### Acknowledgment

The support of the National Natural Science Foundation of China (grant no. 50072013) is gratefully acknowledged.

#### References

1. B. M. KULWICKI, *J. Phys. Chem. Solids* **45** (1984) 1015.
2. C. J. FROSCHE, *Bell Lab. Rec.* **32** (1954) 336.
3. H. F. DIENEL, *ibid.* **34** (1956) 407.
4. S. A. PIANARO, P. R. BUENO, E. LONGO *et al.*, *J. Mater. Sci. Lett.* **14** (1995) 692.
5. E. R. LEITE, J. A. VARELA and E. LONGO, *J. Mater. Sci.* **27** (1992) 5325.
6. M. MATSUOKA, *Jpn. J. Appl. Phys.* **10** (1971) 736.
7. L. M. LEVINSON and H. R. PHILIPP, *J. Appl. Phys.* **46** (1975) 1332.
8. N. YAMAOKA, M. MASUYAMA and M. FUKI, *Amer. Ceram. Bull.* **62** (1983) 698.
9. JIN-FENG WANG, HONGCUN CHEN *et al.*, *Chin. Phys. Lett.* **17** (2000) 530.
10. W. B. SU, J. F. WANG and H. C. CHEN, *J. Appl. Phys.* **92** (2002) 4779.
11. WILLIAM W. COFFEEN, *J. Amer. Ceram. Soc.* **36** (1953) 207.
12. T. K. GUPTA, *ibid.* **73** (1990) 817.
13. DAVID R. CLARKE, *ibid.* **82** (1999) 485.
14. KAZUO EDA, *J. Appl. Phys.* **49** (1978) 2964.
15. J. WONG, *ibid.* **49** (1976) 4971.
16. T. K. GUPTA and W. G. CARLSON, *J. Mater. Sci.* **20** (1985) 3487.
17. H. R. PHILIPP and L. M. LEVINSON, *J. Appl. Phys.* **46** (1975) 3206.

Received 28 March

and accepted 26 September 2003